Sulfide-Bridged Derivatives of the Binuclear Iron Site of Hemerythrin at both Met and Semi-Met Oxidation Levels†

Gudrun S. Lukat, Donald M. Kurtz, Jr.,* Andrew K. Shiemke, Thomas M. Loehr, and Joann Sanders-Loehr

ABSTRACT: Exposure of methemerythrin (metHr) to S^{2-} under anaerobic conditions results in a one-electron reduction to the semi-met level and replacement of the μ-oxo bridge between the irons with a single sulfide. The sulfide bridge is maintained upon ferricyanide oxidation of semi-metsulfide to metsulfide hemerythrin and upon subsequent dithionite or S^{2-} reduction back to the semi-met level. Chemical analyses show that metsulfideHr contains one S^{2-} per two Fe. The single quadrupole doublet (δ = 0.50 mm/s; ΔE_q = 0.99 mm/s) in the Mössbauer spectrum is consistent with a bridging sulfide geometry. The optical and resonance Raman spectra of metsulfideHr are reminiscent of the [2Fe–2S] iron–sulfur proteins. The optical spectrum exhibits multiple $S^{2-} \rightarrow$ Fe(III) charge-transfer transitions between 400 and 600 nm. The resonance Raman spectrum reveals a series of overtones and combinations of the 431-cm^{-1} Fe–S–Fe symmetric vibration and the 327-cm^{-1} asymmetric vibration. The relative energies of the symmetric and asymmetric modes are characteristic of a sulfur-bridged system with a bridge angle of approximately 80°. MetsulfideHr decomposes over several hours in air and over several days in the absence of O_2 to metHr and semi-metsulfideHr, respectively. Unlike metHr and semi-metHr, neither the metsulfide nor the semi-metsulfide derivatives form stable adducts with anions such as azide or cyanide. Sulfide bridging confers new properties on the binuclear iron center that are of interest to an understanding of the chemistry of hemerythrin and also of the [2Fe–2S] iron–sulfur proteins.

Hemerythrin (Hr)[1] is a non-heme oxygen-carrying protein found in several phyla of marine invertebrates. The protein from most organisms consists of an octamer of M_r 108 000, and each of the eight identical subunits contains two iron atoms at a binuclear site that reversibly binds one molecule of oxygen. Extensive chemical and spectroscopic investigations have established that upon oxygenation the two high-spin Fe^{II} ions in deoxyHr are oxidized to Fe^{III} in oxyHr and the bound dioxygen is reduced to the peroxide oxidation state (Kurtz et al., 1977; Sanders-Loehr & Loehr, 1979; Wilkins & Harrington, 1983; Klotz & Kurtz, 1984). MetHr is an oxidized form containing two high-spin Fe^{III} ions, which does not bind oxygen but which does bind several small anions such as N_3^-, SCN^-, CN^-, and Cl^-. MetHr can be converted back to the oxygen binding form with reducing agents. X-ray crystallography shows that metHr has the active site structure shown in Chart I (Stenkamp et al., 1983, 1984). In addition to terminal histidine ligands, two carboxylates from the protein and an oxo ion from water bridge the two irons. The 5-coordinate iron binds added N_3^- as shown, and recent results indicate that dioxygen occupies the same position in oxyHr (R. E. Stenkamp, L. C. Sieker, L. H. Jensen, J. D. McCallum, and J. Sanders-Loehr, unpublished results). Magnetic susceptibility measurements on the oxy and met forms (Dawson et al., 1972) indicate strong antiferromagnetic coupling between the irons ($J \sim -100$ cm^{-1}), leading to a diamagnetic ground state. EXAFS and X-ray crystallographic measurements give an iron–iron distance in the range of 3.2–3.6 Å for oxy- and metHrs (Elam et al., 1982; Hendrickson et al., 1982; Stenkamp et al., 1984). At these distances the antiferromagnetic coupling must occur predominantly through the bridging ligands. Comparisons to synthetic molecules indicate that the strength of the coupling can be entirely accounted for by the presence of the μ-oxo bridge (Murray, 1974). An intermediate $Fe^{II}Fe^{III}$ semi-met oxidation level of Hr can be attained either by reduction to metHr to give so-called $(semi\text{-}met)_R$ or by oxidation of deoxyHr to give $(semi\text{-}met)_O$ (Babcock et al., 1980). EPR spectra of semi-metHr (Muhoberac et al., 1980) are consistent with an $S = {}^1/_2$ ground state, indicating retention of antiferromagnetic coupling.

Chart I

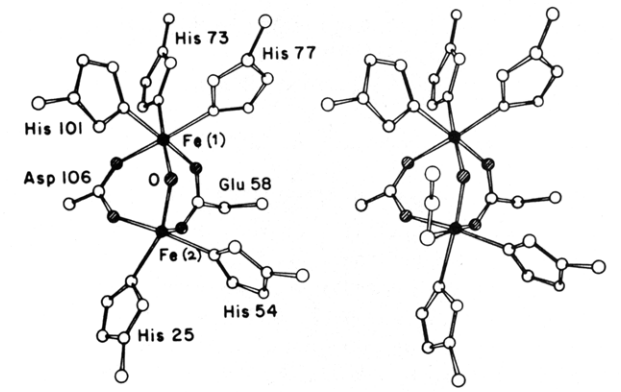

One anticipates that the reaction of metHr with sulfide may be more complex than with the anions mentioned above. Sulfide possesses the well-documented capability of bridging two iron atoms (Mitchell & Parker, 1973; Berg & Holm, 1982; Do et al., 1983) and may also reduce ferric iron. A derivative prepared by addition of sulfide to metHr was first reported in 1965 (Keresztes-Nagy & Klotz) and was isolated in crystalline form in 1970 (Bayer et al.). Resonance Raman spectra of this derivative (Freier et al., 1979) were interpreted in terms of a structure in which a μ-sulfido bridge has replaced the μ-oxo bridge. Recently, Kurtz et al. (1983) showed that this

† From the Department of Chemistry, Iowa State University, Ames, Iowa 50011 (G.S.L. and D.M.K.), the Department of Chemical, Biological and Environmental Sciences, Oregon Graduate Center, Beaverton, Oregon 97006 (A.K.S. and T.M.L.), and the Department of Chemistry, Portland State University, Portland, Oregon 97207 (J.S.-L.). *Received April 17, 1984.* This research was supported by National Science Foundation Grant PCM-8216447 (G.S.L. and D.M.K.) and National Institutes of Health Grant GM 18865 (A.K.S., T.M.L., and J.S.-L.).

[1] Abbreviations: Hr, hemerythrin; EXAFS, extended X-ray absorption fine structure; Tris, tris(hydroxymethyl)aminomethane; salen, *N*,*N*′-methylenebis(salicylideneaminato).

0006-2960/84/0423-6416$01.50/0

sulfide derivative and the corresponding selenide derivative have, in fact, been reduced to the semi-met oxidation level and that the irons remain antiferromagnetically coupled.

We now report that a sulfide derivative of Hr can also be prepared at the met oxidation level. Our evidence supports sulfide replacement of the μ-oxo bridge in both met- and semi-metsulfideHrs. In addition to providing new information on the chemistry of the binuclear iron site in Hr, these sulfide derivatives also display some of the characteristics of [2Fe–2S] sites in iron–sulfur proteins.

Experimental Procedures

Preparation of MetHr. OxyHr was isolated and crystallized from the coelomic fluid obtained from live worms of the species *Phascolopsis gouldii* purchased from Marine Biological Laboratories, Woods Hole, MA (Klotz et al., 1957). MetHr was prepared by dialysis of solutions of oxyHr against 50 mM Tris–perchlorate or Tris–acetate, pH 8.0, containing $K_3Fe(CN)_6$. Excess ferricyanide was then removed by dialysis. All protein concentrations are expressed as monomer and were determined spectrophotometrically, usually as the metazide derivative (Garbett et al., 1969). Reductions of metHr were performed under Ar in septum-capped vials, transferring reagents via gas-tight syringe as described previously (Kurtz et al., 1983). Sodium tetrasulfide (Na_2S_4) was purchased from Alfa and added to metHr from aqueous stock solutions.

Preparation of MetsulfideHr. Except where noted, all operations were carried out at 4 °C under N_2 or Ar. Solutions and dialysis buffers were degassed before use. Reagents were transferred via gas-tight syringe. Two to five milliliters of 1–2 mM metHr in 50 mM Tris–perchlorate or Tris–acetate, pH 8.0, was dialyzed against 1 L of buffer containing 2–3 mM S^{2-} added as either $Na_2S{\cdot}9H_2O$ or NaHS (Eibeck, 1963). After 6–10 h, the dialysis sack containing the purple semi-metsulfideHr was transferred to 1 L of buffer containing 2 mM $K_3Fe(CN)_6$. After ~8 h of dialysis, the ferri- and ferrocyanide were removed by dialysis for a total of ~8 h against two changes of 1 L of buffer or by aerobic passage through a small column of Sephadex G-25. Alternatively, 4 equiv of S^{2-} was added from a stock solution to a solution of metHr. After ~1 h, 4 equiv of $K_3Fe(CN)_6$ was added. Within 2 min the protein solution changed from the purple color of semi-metsulfideHr to the red color of metsulfideHr. The dialysis procedure, though more lengthy, gave more reproducible and reliable preparations.

Analyses. Extinction coefficients based on monomer concentration for the absorption spectrum of metsulfideHr in 50 mM Tris–acetate, pH 8.0, were determined by iron analysis with the *o*-phenanthroline method (Rill & Klotz, 1970). Sulfide concentrations of stock solutions were determined iodometrically (Freier et al., 1979). Sulfide and sulfane (S^0) contents of metsulfideHr were determined by the method of Beinert (1983). Standard curves were determined from stock solutions of $Na_2S{\cdot}9H_2O$. These analyses were done in parallel with iron analyses to obtain a S^{2-} to Fe ratio for the protein. Concentrations of stock solutions of $Na_2S_2O_4$ were determined by titration with solutions of $K_3Fe(CN)_6$, whose concentrations were determined from ϵ_{420} = 1030 M^{-1} cm^{-1} (Irwin et al., 1983).

Spectroscopy. Absorption spectra were obtained on a Perkin-Elmer Model 554 spectrophotometer. Anaerobic samples were placed in double septum sealed quartz cuvettes, which were similar to a previously described design (Averill et al., 1978). EPR spectra were obtained on 0.1-mL aliquots of reaction mixtures contained in 4 mm o.d. quartz tubes that were evacuated and flame sealed. X-band spectra were obtained at 4 K on a Bruker Model ER220D spectrometer equipped with an Oxford ESR-10 helium flow sytem. Copper sulfate was used as the concentration standard for double integration (Aasa & Vänngård, 1975). Mössbauer spectra of 5–10 mM solutions of metsulfideHr in 50 mM Tris–perchlorate, pH 8.0 (concentrated in an Amicon filter with PM-30 membranes), were obtained at the University of Illinois as previously described (Kurtz et al., 1983). Isomer shift is referenced to Fe metal at 300 K. Resonance Raman spectra were collected at the Oregon Graduate Center on a computer-interfaced Jarrell-Ash spectrophotometer equipped with Spectra Physics 164-05 (Ar) and 164-01 (Kr) ion lasers, an RCA C31034 photomultiplier tube, and an ORTEC Model 9302 amplifier/discriminator. Spectra were obtained on solutions of Hr ~2 mM in monomer, which were placed in capillary tubes. Temperature was controlled by flowing cold N_2 gas over the capillary (regulating the rate of boiloff from a Dewar of liquid N_2) or by placing the capillary in the cold-finger of a liquid N_2 dewar (Sjöberg et al., 1982). Thawed solutions of metsulfideHr tended to bleach in the laser beam whereas no bleaching was detected in solutions run at 77 K. In all cases, 180° backscattering geometry was used, and multiple scans were collected and averaged to enhance signal-to-noise ratio. Laser power at the sample ranged from 30 to 130 mW for visible excitation and from 12 to 15 mW for UV excitation. Slit widths of 8–10 cm^{-1} were used. Estimates of peak intensity at various excitation wavelengths were made relative to that of ν_1 of perchlorate at 935 cm^{-1}.

Results and Discussion

Interpretation of the spectroscopic and analytical data together with the pattern of reactivity leads us to the conclusion that a single sulfide has replaced the μ-oxo bridge in semi-metS^{2-} and metS^{2-}. Scheme I summarizes the reactions and states of Hr that are discussed below and defines the abbreviated nomenclature for the various states of Hr used throughout the discussion. In semi-metS^{2-} and (semi-met)$_R$, the assignment of Fe^{III} to the 5-coordinate ion is arbitrary. For reactions run at pH 8.0 in the absence of perchlorate, the form designated met is actually a mixture of met and metOH^- (McCallum et al., 1984).

Characterization of Semi-metS^{2-}. Anaerobic treatment of met with one or more molar equivalents of S^{2-} from stock solutions of $Na_2S{\cdot}9H_2O$ or NaHS results in semi-metS^{2-} (Freier et al., 1979; Kurtz et al., 1983). At 100 K, the Mössbauer spectrum of semi-metS^{2-} consists of two major doublets with δ (ΔE_q) in mm/s of 0.58 (1.58) and 1.14 (2.43) ascribed to high-spin Fe^{III} and Fe^{II} components, respectively (Kurtz et al., 1983). This spectrum broadens substantially either in weak applied fields or at 4.2 K, indicative of a paramagnetic center. The EPR spectrum with g = 1.88, 1.71, and 1.40 is typical of an antiferromagnetically coupled $S = {}^1/_2$ system. This signal has now been quantitated as one spin per two Fe. The combined Mössbauer and EPR data show that this derivative is at the semi-met oxidation level.

The absorption spectrum of semi-metS^{2-} contains a prominent shoulder at 340 nm and a broad maximum in the visible region at ~500 nm (Figure 1). The resonance Raman spectrum of semi-metS^{2-} obtained with 363.8-nm excitation (Figure 2, insert) is identical with that obtained by Freier et al. (1979) with 514.5-nm excitation. They assigned the peak at 444-cm^{-1} to the symmetric vibration of an Fe–S–Fe moiety on the basis of the agreement between calculated and observed ^{34}S isotope shifts and the lack of a deuterium isotope effect. We find that this peak is approximately 5-fold more intense with UV than with 514.5-mm excitation, indicating that the

Scheme I

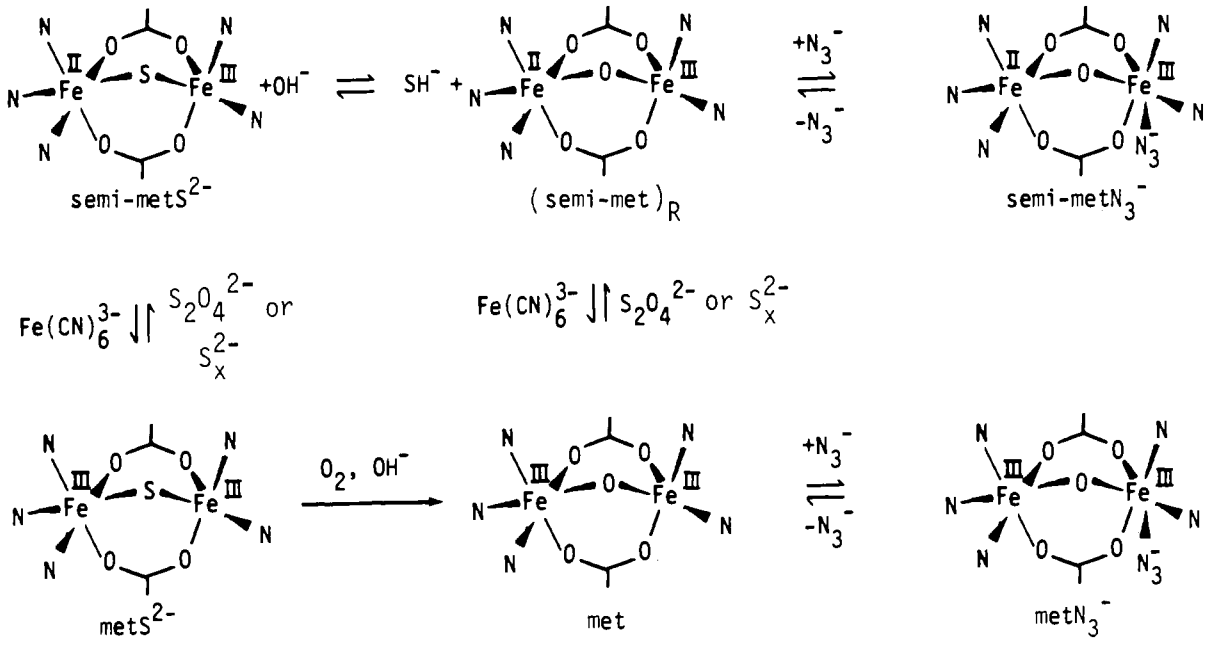

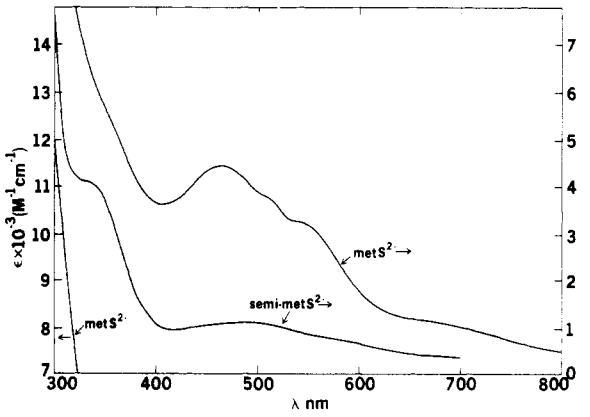

FIGURE 1: Absorption spectra of met and semi-metsulfideHrs in anaerobic 50 mM Tris–acetate, pH 8.0.

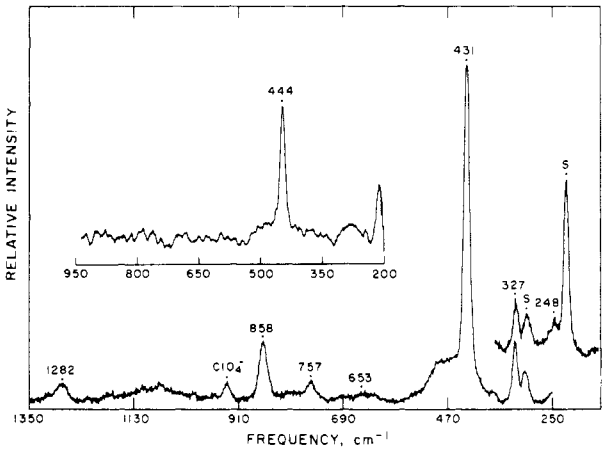

FIGURE 2: Resonance Raman spectra of 2 mM metsulfideHr in 50 mM Tris–perchlorate, pH 8.0. The solution contains ~0.4 M $NaClO_4$ as an internal standard. Conditions were as follows: temperature 77 K; excitation 488.0 nm, 130 mW; scan rate 1 cm^{-1}/s; slit width 8 cm^{-1}; 34 scans averaged. Peaks at 223 and 307 cm^{-1} labeled S in a 5:1 intensity ratio are characteristic of frozen solvent at 77 K. The broad feature between 450 and 500 cm^{-1} is due to glass. (Insert) Resonance Raman spectrum of 2 mM semi-metsulfideHr in 50 mM Tris–perchlorate, pH 8.0. Conditions were as follows: temperature 243 K; excitation 363.8 nm, 12 mW; scan rate 1 cm^{-1}/s; slit width 8 cm^{-1}; 11 scans averaged.

absorption band at 340 nm has considerable $S^{2-} \rightarrow$ Fe charge-transfer character.

Although semi-metS^{2-} is the ultimate product, samples frozen within a few minutes of mixing S^{2-} with met contain both semi-metS^{2-} and $(\text{semi-met})_R$ EPR signals, the latter with $g = 1.93$, 1.86, and 1.68 (Babcock et al., 1980). Prolonged anaerobic dialysis of semi-metS^{2-} also results in such mixtures. Addition of 1 reducing equivalent of $Na_2S_2O_4$/mol of met to give $(\text{semi-met})_R$ followed by addition of excess S^{2-} gives quantitative formation of the semi-metS^{2-} EPR signal when compared to the integrated intensity of the $(\text{semi-met})_R$ EPR signal prior to addition of S^{2-}. These results indicate that the pathway for semi-metS^{2-} formation proceeds via initial reduction of met to semi-met, with bridge exchange occurring at the semi-met level, and that the exchange is reversible as indicated in Scheme I. The same sequence was previously observed for formation of the semi-metSe^{2-} derivative (Kurtz et al., 1983).

We have obtained complete conversion to semi-metS^{2-}, as judged by EPR intensity, upon addition of ~1 mol of S^{2-}/mol of met. One possible source of additional reducing equivalents could be polysulfide species present in stock solutions of S^{2-}. Na_2S_4 at a ratio of ~0.25 mol/mol of met causes quantitative reduction of met to $(\text{semi-met})_R$ as judged by double integration of the characteristic EPR signal. Larger ratios of Na_2S_4 result in EPR spectra consisting of a mixture of those due to $(\text{semi-met})_R$ and semi-metS^{2-}. Polysulfides are also likely to be generated during the reduction of met by S^{2-}. The presence of polysulfides and their ability to cause reduction to semi-met make titrations of met with S^{2-} difficult to quantitate in terms of S^{2-}/Fe stoichiometry.

The spectroscopically distinct form $(\text{semi-met})_O$, which is produced by one-electron oxidation of deoxyHr with $Fe(CN)_6^{3-}$, shows a distinctive behavior with S^{2-}. Instead of forming semi-metS^{2-} as is the case with $(\text{semi-met})_R$, treatment of $(\text{semi-met})_O$ with S^{2-} results in its reduction back to deoxyHr. The differential behavior of $(\text{semi-met})_O$ and $(\text{semi-met})_R$ toward oxidizing and reducing agents has been noted previously (Babcock et al., 1980). The pattern of reactivity with sulfide is clearly distinguished from that with other anions, such as N_3^-, where the identical semi-metN_3^-

adduct is formed from either $(semi\text{-}met)_O$ or $(semi\text{-}met)_R$.

Characterization of MetS²⁻. Treatment of semi-metS²⁻ with $Fe(CN)_6^{3-}$ under anaerobic conditions results in metS²⁻. Sulfide and iron analyses were carried out in parallel to establish the stoichiometry in metS²⁻ after dialysis to remove excess S^{2-}. These analyses gave a ratio of 0.89 ± 0.11 S^{-2} per two Fe (average of nine determinations) while sulfide plus sulfane analyses gave a ratio of 0.97 ± 0.08 (S^{2-} + S^0) per two Fe (average of five determinations). These results indicate that one S^{2-} per two Fe is the correct ratio in metS²⁻ and that no significant amounts of persulfide (S_2^{2-}) or sulfane sulfur are present.

Oxidation of semi-metS²⁻ to metS²⁻ results in increased absorbance throughout the visible and near-UV region (Figure 1). The spectral parameters, λ (ϵ_M), for metS²⁻ are 464 nm (4500), 516 nm (sh), 540 nm (sh) (3300), and 680 nm (sh) (1200). The ~4-fold increase in absorbance of the main visible transition upon conversion of semi-metS²⁻ (ϵ_{500} 1100 M^{-1} cm^{-1}; Freier et al., 1979) to metS²⁻ is similar to that observed upon oxidation of the [2Fe–2S] protein adrenodoxin (Yachandra et al., 1983) and contrasts with the ~1.5-fold increase in absorbance of the main visible transition upon conversion of semi-metN_3^- to metN_3^- (Wilkins & Harrington, 1983; Garbett et al., 1969). However, the more significant difference between spectra of metS²⁻ and those of the oxo-bridged species appears in the near-UV region. Spectra of oxyHr, met, all other anion adducts of met, and a synthetic analogue of met contain two intense peaks (ϵ ~6000–10 000 M^{-1} cm^{-1}) at ~320 and ~360 nm, one or both of which have been assigned to bridging $O_2^{-} \rightarrow$ Fe charge transfer (Garbett et al., 1969; Solomon, 1981; Shiemke et al., 1984; Armstrong et al., 1984). The absence of well-resolved near-UV bands from the spectrum of metS²⁻ is further evidence against the presence of a μ-oxo bridge at the iron site.

MetS²⁻ gives no EPR spectrum at 4 or 77 K. The Mössbauer spectrum at 100 K in an applied magnetic field of 1.7 kG consists of a single doublet, each component of which is ~0.34 mm/s wide at half-height. The quadrupole splitting, ΔE_q, is 0.99 mm/s and the isomer shift, δ, is 0.50 mm/s. No significant differences are observed at 4.2 K. The isomer shift and the lack of significant broadening in a weak applied field or at low temperature are different from the behavior of semi-metS²⁻ (vide supra) and together with the lack of an EPR spectrum are characteristic of Hr at the met oxidation level, i.e., of an antiferromagnetically coupled pair of high-spin Fe^{III} ions (Garbett et al., 1969). The value of ΔE_q for metS²⁻ is about 40% smaller than that of met. A similar trend is observed in the Mössbauer spectra of $[Fe(salen)]_2X$, X = O or S, where replacement of the μ-oxo bridge by a μ-sulfido bridge gives almost no change in δ but a significant reduction in ΔE_q (Mitchell & Parker, 1973). The fact that only a single quadrupole doublet is obtained for metS²⁻ further supports a bridging sulfide geometry. The μ-oxo-bridged met form, having both 5- and 6-coordinate iron atoms (Stenkamp et al., 1984), also shows only a single quadrupole double with δ = 0.46 mm/s and ΔE_q = 1.57 mm/s (Garbett et al., 1969). One would expect unequal perturbations of these two irons if S^{2-} were to bind to only one of them.

The resonance Raman spectrum of metS²⁻ is strikingly different from that of semi-metS²⁻ in that it contains at least seven resonance-enhanced vibrational modes (Figure 2). Analysis of the frequencies indicates that the peaks at 653, 757, 858, and 1282 cm^{-1} represent overtones and combinations of fundamentals at 327 and 431 cm^{-1} (Table I). Similar frequency progressions have been observed in the resonance Raman spectra of oxidized but not reduced [2Fe–2S] iron–sulfur proteins (Yachandra et al., 1983), as also appears to be the case for metS²⁻ vs. semi-metS²⁻. In every other anion adduct of met so far examined (Kurtz et al., 1977; Freier et al., 1980), the symmetric stretching vibration of the Fe–O–Fe unit appears at ~500 cm^{-1} in the resonance Raman spectrum. The absence of the 500-cm^{-1} band in the resonance Raman spectrum of metS²⁻ is further evidence against a system having a μ-oxo bridge and a terminally bound sulfide in this form of the protein.

Table I: Resonance Raman Vibrational Frequencies and Assignments for MetsulfideHr and Semi-metsulfideHr

frequency (cm^{-1})	assignment
MetsulfideHr	
327	ν_{as}(Fe–S–Fe)
431	ν_s(Fe–S–Fe)
653	$2\nu_{as}$
757	$\nu_{as} + \nu_s$
858	$2\nu_s$
1282	$3\nu_s$
Semi-metsulfideHr	
444	ν_s(Fe–S–Fe)[a]

[a] Freier et al., 1979.

The 431-cm^{-1} fundamental in the resonance Raman spectrum of metS²⁻ is assigned as the symmetric Fe–S–Fe stretching vibration since totally symmetric modes generally show the greatest Raman intensities and resonance enhancements (Spiro & Stein, 1977). The 327-cm^{-1} fundamental is assigned to an Fe–S–Fe asymmetric vibration by analogy to the vibrational modes in the Fe_2S_2 unit: ν_s at ~400 cm^{-1}; ν_{as} at ~420 (w), ~370 (w), and ~290 (s) cm^{-1} (Yachandra et al., 1983). The occurrence of an asymmetric mode at a lower energy than the symmetric mode is indicative of a small Fe–S–Fe angle (Wing & Callahan, 1969) as in the Fe_2S_2 clusters where Fe–S–Fe ≃ 75° (Berg & Holm, 1982). Although met has an Fe–O–Fe angle of 127° (Stenkamp et al., 1984), substitution of S for O is expected to result in an ~0.35-Å lengthening of each of the bridge bonds Berg & Holm, 1982; Stenkamp et al., 1984). If the iron atoms in metS²⁻ are constrained by the protein so that the geometric change associated with sulfur replacement of the oxo bridge occurs at the sulfur atom, the resulting Fe–S–Fe angle is calculated to be ~98°. By use of the secular equations of Wing & Callahan (1969) for an Fe–S–Fe system, good agreement with the observed ν_3(Fe–S–Fe) and ν_{as}(Fe–S–Fe) of metS²⁻ can be achieved with values of 172 N m^{-1} for the Fe–S stretching force constant, 27 N m^{-1} for the bending force constant, and 79.6° for the Fe–S–Fe bridge angle. The value for the bending force constant is similar to that established by Yachandra et al. 1983) for the Fe_2S_2 system, whereas the value for the stretching force constant is ~30 N m^{-1} higher, which is reasonable for a single sulfur bridge.

The 13-cm^{-1} decrease in ν_s(Fe–S–Fe) in metS²⁻ relative to semi-metS²⁻ is surprising. In adrenodoxin, for example, a one-electron oxidation results in 16–24-cm^{-1} increases in bridge stretching vibrations (Yachandra et al., 1983) as expected for increased bond strengths at higher oxidation states. In metS²⁻, structural or electronic changes accompanying oxidation must be compensating for the increase in the net charge of the complex. A similar conclusion has been reached in the comparison of oxyHr and met where ν_s(Fe–O–Fe) differs by ~20 cm^{-1} without any change in the formal oxidation states of the iron atoms (Shiemke et al., 1984).

The Raman intensities of both the 431-cm^{-1} and 327-cm^{-1} bands relative to the perchlorate internal standard varied with

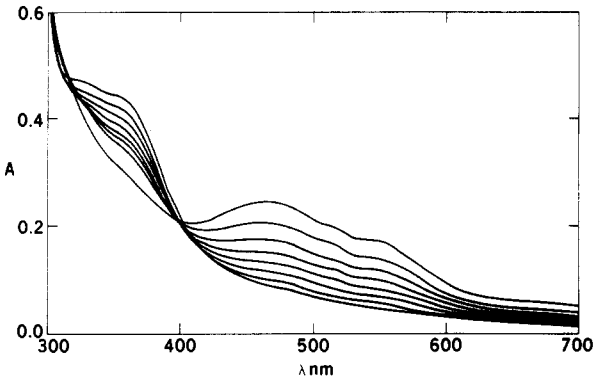

FIGURE 3: Absorption spectra observed during aerobic incubation of 53.9 μM metsulfideHr in 50 mM Tris–perchlorate, pH 8.0, at room temperature. Path length = 1 cm. With time, the spectra show a decrease in absorbance at 464 nm and an increase at 360 nm. The second scan was recorded 4 h after the initial scan. Succeeding spectra are at ~1-h intervals.

excitation wavelength in the order 488.0 nm > 530.9 nm > 406.7 nm. Transitions at ~450 and ~570 nm in the absorption spectra of [2Fe–2S] ferredoxins and their synthetic analogues have been assigned to bridging $S^{2-} \rightarrow Fe^{III}$ charge transfer on the basis of Raman excitation profiles. The intensity variation in the Raman spectra of $metS^{2-}$ is consistent with a similar assignment for its visible absorption spectrum and, in particular, the maximally absorbing component at 464 nm (Figure 1).

Stability and Reactivity of $MetS^{2-}$. In the presence of O_2, $metS^{2-}$ is unstable relative to met. The binuclear iron center of $metS^{2-}$ slowly reverts to the oxo-bridged configuration (Scheme I), accompanied apparently by oxidation of S^{2-}. This conversion can be followed spectrophotometrically. In *aerobic* Tris–perchlorate, pH 8.0, at room temperature the absorption spectrum of $metS^{2-}$ changes smoothly over the course of ~12 h to that of met with isosbestic points at ~400 and ~320 nm (Figure 3). A slight turbidity develops during the latter stages of the reaction attributable to precipitation of S^0. The protein product is confirmed by addition of excess N_3^-, which results in the characteristic absorption spectrum of $metN_3^-$ (N_3^- does not react rapidly with $metS^{2-}$). Examinations of 0.1-mL aliquots of the reaction mixture show that the $metS^{2-} \rightarrow$ met transformation is not accompanied by the development of any significant EPR intensity at 4 K. In aerobic Tris–acetate, pH 8.0, the same $metS^{2-} \rightarrow$ met transformation occurs in ~6 h at room temperature.

In contrast to the aerobic behavior, a much slower $metS^{2-} \rightarrow$ semi-$metS^{2-}$ transformation occurs in the absence of O_2. In *anaerobic* Tris–perchlorate, pH 8.0, $metS^{2-}$ is stable for several days at 4 °C and for much longer when frozen. At room temperature in anaerobic Tris–perchlorate, pH 8.0, no significant changes in the absorption spectrum of $metS^{2-}$ occur for ~6 h. However, over the course of 3 days at room temperature a shoulder at 340 nm, a decrease in visible absorbance, and an EPR spectrum (Figure 4), which are all characteristic of semi-$metS^{2-}$, develop. The maximum integrated area of the semi-$metS^{2-}$ EPR spectrum is 0.8 spin per two Fe for this autoreduction. Under these conditions, this reaction occurs to the same extent in about half the time in Tris–acetate, pH 8.0. One possibility is that this transformation proceeds by dissociation of 20% of the S^{2-} followed by reduction of the remaining 80% of $metS^{2-}$ by the dissociated S^{2-}. This possibility is lent support by the result that addition of S^{2-} to $metS^{2-}$ results in immediate reduction to semi-$metS^{2-}$.

When an aerobic solution of $metS^{2-}$ is incubated in the presence of an ~500-fold molar excess of N_3^-, the characteristic EPR (Figure 5) and UV–vis spectra of semi-$metN_3^-$ (Babcock et al., 1980; Wilkins & Harrington, 1983) develop over the course of ~10 h. As indicated in the legend to Figure 5, double integration of the semi-$metN_3^-$ EPR signals show that this transformation is quantitative. At longer reaction times than those shown in Figure 5, conversion to $metN_3^-$ is indicated in aerobic solutions by a decrease in EPR intensity and by development of the characteristic UV–vis spectrum (Garbett et al., 1969). The fact that the $metS^{2-} \rightarrow$ semi-$metN_3^-$ reaction is completed within ~10 h suggests that although N_3^- does not appear to form a stable complex with $metS^{2-}$ it does facilitate the reductive decomposition of $metS^{2-}$ to the semi-met level.

Reaction of $Na_2S_2O_4$ with $metS^{2-}$ mimics the fast reduction of $metS^{2-}$ by S^{2-}. Addition of 1 reducing equivalent of $Na_2S_2O_4$/mol of $metS^{2-}$ gives quantitative formation of the semi-$metS^{2-}$ EPR signal within 1 min after mixing. As shown in Scheme I, these relatively rapid reductions are more consistent with bridging than terminal sulfide on the basis of

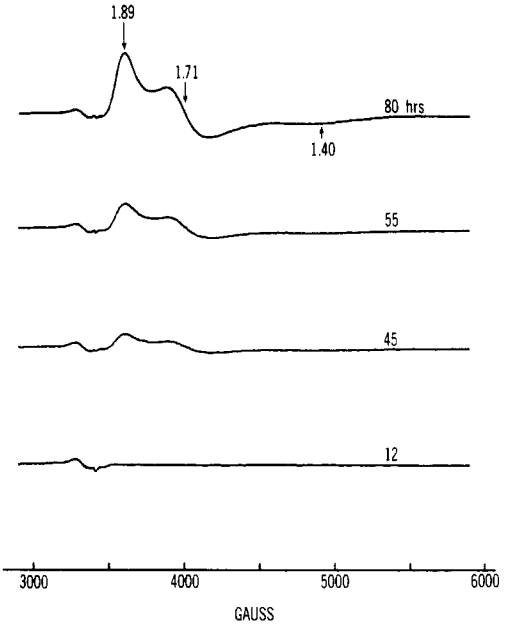

FIGURE 4: EPR spectra observed at the indicated times during anaerobic incubation at room temperature of 1.78 mM metsulfideHr in 50 mM Tris–perchlorate, pH 8.0. EPR conditions were as follows: temperature 4 K; frequency 9.57 GHz; power 100 μW; modulation 16 G at 100 kHz; time constant 0.2 s; receiver gain 3.2×10^4. Double integration gives the following spins per two Fe: 12 h, 0; 45 h, 0.04; 55 h, 0.14; 80 h, 0.81. The weak feature at ~3300 G is from the EPR cavity.

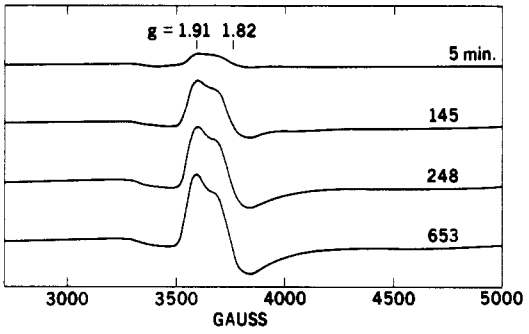

FIGURE 5: EPR spectra observed at the indicated times during aerobic incubation at room temperature of 1.41 mM metsulfideHr in 50 mM Tris–acetate, pH 8.0, in the presence of 0.76 M NaN_3. EPR conditions were as follows: temperature 4 K; frequency 9.57 GHz; power 100 μW; modulation 16 G at 100 kHz; time constant 0.2 s; receiver gain 4×10^4. Double integration gives the following spins per two Fe: 5 min, 0.14; 145 min, 0.41; 248 min, 0.85; 653 min, 1.0.

analogies to the corresponding μ-oxo bridged derivatives. For terminal anion adducts of met such as $metN_3^-$, only the dissociated form reacts with reducing agents, and the reactions occur over much longer time periods (Olivas et al., 1979).

Addition of a 100-fold molar excess N_3^-, SCN^-, CN^-, or Cl^- to solutions of $metS^{2-}$ in either Tris–perchlorate or Tris–acetate buffer, pH 8.0, fails to significantly perturb the absorption spectrum of $metS^{2-}$ for at least 1 h at 4 °C. Similarly, the resonance Raman spectrum of $metS^{2-}$ in Tris–perchlorate, pH 8.0, is unperturbed even after several hours of incubation at 4 °C in the presence of excess N_3^- except for the presence of a weak peak at 371 cm^{-1}, indicative of a small proportion of $metN_3^-$ (Irwin et al., 1983). Thus, added anions fail to bind to $metS^{2-}$ at least on the time scale at which they are known to bind to met (Meloon & Wilkins, 1976). Anions also fail to bind to the iron site of semi-$metS^{2-}$ (Frier et al., 1979).

For Fe^{III}–sulfide, there are far fewer examples of terminal than bridging sulfide geometries (Berg & Holm, 1982; Mitchell & Parker, 1973; Do et al., 1983). The spectroscopic and analytical data, the differences in reactivities of met and semi-met with S^{2-} compared to those with N_3^-, and the similarities in reactivities of $metS^{2-}$ and met with $Na_2S_2O_4$ and with S^{2-} are all fully consistent with a single sulfide replacing the μ-oxo bridge in the sulfideHrs. Assuming this latter geometry, the absence or extreme slowness of anion addition to the iron site of $metS^{2-}$ compared to that of met can be rationalized on both steric and electronic grounds. Replacement of the bridging oxygen with the more electron-donating sulfur could reduce the tendency of the 5-coordinate iron to add a sixth ligand, especially an anion. Sulfur-containing ligands to iron most often stabilize less than 6-coordination (Berg & Holm, 1982). Evidence accumulated over several years has shown that the anion coordination site in metHr is sterically restricted to ligands consisting of three or fewer non-hydrogen atoms (Garbett et al., 1969; Kurtz et al., 1977; Wilkins & Harrington, 1983). Upon substitution of bridging sulfide for oxide, the increase in bridge bond distances discussed above coupled with the larger ionic radius of sulfide could result in increased steric restrictions at the anion binding site.

Lowered anion affinity is also observed with met in the presence of perchlorate ion (Meloon & Wilkins, 1976; Bradić & Wilkins, 1983). In this case, X-ray diffraction results (Stenkamp et al., 1983) indicate that binding of ClO_4^- to the surface of the molecule induces a slight structural change close to the site where anions bind to iron. Thus, the ability of the binuclear iron site in Hr to react with exogenous ligands is quite sensitive to small changes in protein conformation. The slower rates of aerobic oxidation and anaerobic autoreduction of $metS^{2-}$ in perchlorate relative to that in acetate may again be a reflection of the tendency of perchlorate to limit the accessibility of the iron center to anions. Conversely, the increased rate of degradation of $metS^{2-}$ in the presence of azide suggests that this anion binds at a different protein site (presumably at the iron) and thereby lowers the stability of the $metS^{2-}$ derivative.

Conclusions

Scheme I summarizes the structures, reactivities, and probable reaction pathways of $metS^{2-}$ and semi-$metS^{2-}$ at pH 8.0. Most of the interconversions must be performed under anaerobic conditions. The lack of reversibility in the $metS^{2-} \rightarrow$ met step explains why $metS^{2-}$ was not discovered previously; it can be prepared only via oxidation of semi-$metS^{2-}$. Despite the structures depicted in Scheme I, there is as yet no direct evidence for a μ-oxo bridge in $(semi\text{-}met)_R$ or semi-$metN_3^-$. However, our conclusions regarding the μ-sulfido bridges in $metS^{2-}$ and semi-$metS^{2-}$ tend to support the idea that a μ-oxo bridge persists at the semi-met oxidation level in the absence of S^{2-} and that it is more labile than at the met level.

Some interesting parallels can be drawn between the iron sites in the sulfideHrs and [2Fe–2S] centers in iron–sulfur proteins. The oxidation levels of $metS^{2-}$ and semi-$metS^{2-}$ correspond to oxidized and reduced [2Fe–2S] centers, respectively. Both $metS^{2-}$ and oxidized [2Fe–2S] centers consist of an antiferromagnetically coupled pair of high-spin Fe^{III} ions and an $S = 0$ ground spin state. Both semi-$metS^{2-}$ and reduced [2Fe–2S] centers have a trapped valence $Fe^{II}Fe^{III}$ configuration and an $S = {}^1/_2$ ground state (Kurtz et al., 1983; Berg & Holm, 1982). We have been unable to reduce semi-$metS^{2-}$ with retention of S^{2-}, and correspondingly, no "superreduced" [2Fe–2S] center having two Fe^{II} has yet been identified. One would not expect exact parallels in physical or chemical properties between the $Fe_2S(O_2CR)_2$ core of the sulfideHrs and the Fe_2S_2 core of [2Fe–2S] ferredoxins, especially since most of the latter cores are known or suspected to be attached to the protein exclusively via two terminal thiolate ligands per iron (Berg & Holm, 1982). However, our work demonstrates that a stable iron–sulfur center can exist in a protein without thiolate ligation to iron and raises the possibility that such centers naturally occur in as yet undiscovered proteins. Recently, a new "Rieske"-type [2Fe–2S] iron–sulfur protein from *Thermus thermophilus* has been reported that contains equimolar cysteine and iron (Fee et al., 1984). Thus, in this protein at least one terminal ligand per iron must be other than cysteine thiolate. The visible spectrum of this protein in the oxidized form bears a striking resemblance to that of $metS^{2-}$.

Acknowledgments

We thank J. Tim Sage and Dr. Peter Debrunner for obtaining the Mössbauer spectra and for helpful discussions.

Registry No. Fe, 7439-89-6.

References

Aasa, R., & Vänngård, T. (1975) *J. Magn. Reson. 19*, 308–315.

Armstrong, W. H., Spool, A., Papaefthymiou, G. C., Frankel, R. B., & Lippard, S. J. (1984) *J. Am. Chem. Soc. 106*, 3653–3666.

Averill, B. A., Bale, J. R., & Orme-Johnson, W. H. (1978) *J. Am. Chem. Soc. 100*, 3034–3043.

Babcock, L. M., Bradić, Z., Harrington, P. C., Wilkins, R. G., & Yoneda, G. S. (1980) *J. Am. Chem. Soc. 102*, 2849–2850.

Bayer, E., Krauss, P., & Schretzmann, P. (1970) *Z. Naturforsch., B: Anorg. Chem., Org. Chem., Biochem., Biophys., Biol. 25B* 327–328.

Beinert, H. (1983) *Anal. Biochem. 131*, 373–378.

Berg, J. M., & Holm, R. H. (1982) in *Iron-Sulfur Proteins* (Spiro, T. G., Ed.) pp 1–66, Wiley, New York.

Bradić, Z., & Wilkins, R. G. (1983) *Biochemistry 22*, 5396–5401.

Bradić, Z., Harrington, P. C., Wilkins, R. G., & Yoneda, G. S. (1980) *Biochemistry 19*, 4149–4415.

Dawson, J. W., Gray, H. B., Hoenig, H. E., Rossman, G. R., Schredder, J. M., & Wang, R. H. (1972) *Biochemistry 11*, 461–465.

Do, Y., Simhan, E. D., & Holm, R. H. (1983) *Inorg. Chem. 22*, 3809–3812.

Eibeck, R. E. (1963) *Inorg. Synth. 7*, 128–131.

Elam, W. T., Stern, E. A., McCallum, J. D., & Sanders-Loehr, J. (1982) *J. Am. Chem. Soc. 104*, 6369–6373.

Fee, J. A., Findling, K. L., Yoshida, T., Hille, R., Tan, G. E., Hearshen, D. O., Dunham, W. R., Day, E. P., Kent, T. P., & Münck, E. (1984) *J. Biol. Chem. 259*, 124–133.
Freier, S. M., Duff, L. L., VanDuyne, R. P., & Klotz, I. M. (1979) *Biochemistry 18*, 5372–5377.
Freier, S. M., Duff, L. L., Shriver, D. F., & Klotz, I. M. (1980) *Arch. Biochem. Biophys. 205*, 449–463.
Garbett, K., Darnall, D. W., Klotz, I. M., & Williams, R. J. P. (1969) *Arch. Biochem. Biophys. 135*, 419–434.
Harrington, P. C., deWaal, D. J. A., & Wilkins, R. G. (1978) *Arch. Biochem. Biophys. 191*, 444–451.
Hendrickson, W. A., Co, M. S., Smith, J. L., Hodgson, K. O., & Klippenstein, G. L. (1982) *Proc. Natl. Acad. Sci. U.S.A. 79*, 6255–6259.
Irwin, M. J., Duff, L. L., Shriver, D. F., & Klotz, I. M. (1983) *Arch. Biochem. Biophys. 224*, 473–478.
Keresztes-Nagy, S., & Klotz, I. M. (1965) *Biochemistry 4*, 919–931.
Klotz, I. M., & Kurtz, D. M., Jr. (1984) *Acc. Chem. Res. 17*, 16–22.
Klotz, I. M., Klotz, T. A., & Fiess, H. A. (1957) *Arch. Biochem. Biophys. 68*, 284–299.
Kurtz, D. M., Jr., Shriver, D. F., & Klotz, I. M. (1977) *Coord. Chem. Rev. 24*, 145–178.
Kurtz, D. M., Jr., Sage, J. T., Hendrich, M., Debrunner, P. G., & Lukat, G. S. (1983) *J. Biol. Chem. 258*, 2115–2117.
McCallum, J. D., Shiemke, A. K., & Sanders-Loehr, J. (1984) *Biochemistry 23*, 2819–2825.
Meloon, D. R., & Wilkins, R. G. (1976) *Biochemistry 15*, 1284–1290.
Mitchell, P. C. H., & Parker, D. A. (1973) *J. Inorg. Nucl. Chem. 35*, 1385–1390.
Muhoberac, B. B., Wharton, D. C., Babcock, L. M., Harrington, P. C., & Wilkins, R. G. (1980) *Biochim. Biophys. Acta 626*, 337–345.
Murray, K. S. (1974) *Coord. Chem. Rev. 12*, 1–35.
Olivas, E., deWaal, D. J. A., & Wilkins, R. G. (1979) *J. Inorg. Biochem. 11*, 205–212.
Rill, R. L., & Klotz, I. M. (1970) *Arch. Biochem. Biophys. 136*, 507–514.
Sanders-Loehr, J., & Loehr, T. M. (1979) *Adv. Inorg. Biochem. 1*, 235–252.
Shiemke, A. K., Loehr, T. M., & Sanders-Loehr, J. (1984) *J. Am. Chem. Soc.* (in press).
Sjöberg, B.-M., Loehr, T. M., & Sanders-Loehr, J. (1982) *Biochemistry 21*, 96–102.
Solomon, E. I., Eickman, N. C., Gay, R. R., Penfield, K. W., Himmelwright, R. S., & Loomis, L. D. (1981) in *Invertebrate Oxygen Binding Proteins, Structure, Active Site and Function* (Lamy, J., & Lamy, J., Eds.) pp 487–502, Marcel-Dekker, New York.
Spiro, T. G., & Stein, P. (1977) *Annu. Rev. Phys. Chem. 28*, 501–521.
Stenkamp, R. E., Sieker, L. C., & Jensen, L. H. (1983) *J. Inorg. Biochem. 19*, 247–253.
Stenkamp, R. E., Sieker, L. C., & Jensen, L. H. (1984) *J. Am. Chem. Soc. 106*, 618–622.
Wilkins, R. G., & Harrington, P. C. (1983) *Adv. Inorg. Biochem. 5*, 51–85.
Wing, R. M., & Callahan, K. P. (1969) *Inorg. Chem. 8*, 871–874.
Yachandra, V. K., Hare, J., Gewirth, A., Czernuszewicz, R. S., Kimura, T., Holm, R. H., & Spiro, T. G. (1983) *J. Am. Chem. Soc. 105*, 6462–6468.

L-Carnitine Dissimilation in the Gastrointestinal Tract of the Rat†

Charles J. Rebouche,* Diane L. Mack, and Paul F. Edmonson

ABSTRACT: Results of previous studies in this laboratory and others have suggested that L-carnitine is degraded in the gastrointestinal tract of the rat, perhaps by the action of indigenous flora. L-[*methyl*-^{14}C]Carnitine was administered to rats either orally or intravenously in doses of 86 nmol or 124 μmol, and expired air, 48-h urine and fecal collections, and selected tissues at 48 h after isotope administration were examined for radiolabeled carnitine and metabolites. Urine and feces of rats receiving oral L-[*methyl*-^{14}C]carnitine consistently contained two radiolabeled metabolites which were identified as trimethylamine *N*-oxide (primarily in urine) and γ-butyrobetaine (primarily in feces). In these rats, these metabolites accounted for up to 23% and 31% of the administered dose, respectively. By contrast, for rats receiving intravenous L-[*methyl*-^{14}C]carnitine or germ-free rats receiving the isotope orally or intravenously, virtually all of the radioactivity recovered was in the form of carnitine. Analyses for $^{14}CO_2$ and [^{14}C]trimethylamine in expired air revealed little or no (less than 0.1% of dose) conversion to these compounds, regardless of size of dose or route of administration. Results of this study demonstrate conclusively that L-carnitine is degraded in the gastrointestinal tract of the rat and that indigenous flora are responsible for these transformations.

L-Carnitine [β-hydroxy-γ-(*N*-trimethylammonio)butyrate] is a natural constituent of higher organisms and, in particular, cells of animal origin. Its primary function is to transfer long-chain fatty acids, as acylcarnitine esters, across the mitochondrial inner membrane. L-Carnitine is found in many foodstuffs and is particularly abundant in meat and dairy products. This compound is synthesized endogenously from lysine and methionine.

In mammals, carnitine is excreted primarily in urine. Greater than 95% of total carnitine excreted in urine and feces of dogs or humans was present in urine (Rebouche & Engel, 1983, 1984). Carnitine metabolism in rats (Cederblad &

† From the Department of Neurology, Mayo Foundation, Rochester, Minnesota 55905. *Received May 29, 1984.* This study was supported by U.S. Public Health Service Grant AM 27451 and by a Research Center Grant from the Muscular Dystrophy Association.

* Address correspondence to this author at the Department of Pediatrics, University of Iowa College of Medicine, Iowa City, IA 52242.

0006-2960/84/0423-6422$01.50/0